



**HAL**  
open science

# Contribution to the Percolation Threshold Study of Silicon Carbide Filled Polydimethylsiloxane Composites Used For Field Grading Application

Renaud Metz, Hocine Merini, Jean-Michel Reboul, Jean-Louis Bantignies,  
Mehrdad Hassanzadeh

► **To cite this version:**

Renaud Metz, Hocine Merini, Jean-Michel Reboul, Jean-Louis Bantignies, Mehrdad Hassanzadeh. Contribution to the Percolation Threshold Study of Silicon Carbide Filled Polydimethylsiloxane Composites Used For Field Grading Application. *Silicon*, 2023, 15, pp.5297-5305. 10.1007/s12633-023-02424-4 . hal-04118312

**HAL Id: hal-04118312**

**<https://hal.science/hal-04118312>**

Submitted on 5 Feb 2024

**HAL** is a multi-disciplinary open access archive for the deposit and dissemination of scientific research documents, whether they are published or not. The documents may come from teaching and research institutions in France or abroad, or from public or private research centers.

L'archive ouverte pluridisciplinaire **HAL**, est destinée au dépôt et à la diffusion de documents scientifiques de niveau recherche, publiés ou non, émanant des établissements d'enseignement et de recherche français ou étrangers, des laboratoires publics ou privés.

# Contribution to the percolation threshold study of Silicon Carbide filled polydimethylsiloxane composites used for field grading application

Renaud Metz (✉ [renaud.metz@gmail.com](mailto:renaud.metz@gmail.com))

UMR 5221 CNRS-Université de Montpellier

Hocine Merini

UMR 5221 CNRS-Université de Montpellier

Jean-Michel Reboul

Université de Caen Normandie

Jean-Louis Bantignies

UMR 5221 CNRS-Université de Montpellier

Mehrdad Hassanzadeh

Quai Paul Louis Merlin



---

## Research Article

**Keywords:** Silicon Carbide, Silicone, Nonlinear composite material, Field grading material

**Posted Date:** March 27th, 2023

**DOI:** <https://doi.org/10.21203/rs.3.rs-2718564/v1>

**License:**   This work is licensed under a Creative Commons Attribution 4.0 International License. [Read Full License](#)

---

# Abstract

Nonlinear V-I characteristics of particulate composite prepared from dispersion of silicon carbide in a siloxane elastomer have been measured as a function of filler concentration up to the maximum allowable of about 32 vol.%. Two critical concentrations (percolation thresholds) are obtained at volume fractions of about 17 and 24 vol.% for low and high electric fields. These values are consistent with the critical concentrations predicted by the theory: 14 and 31 vol.% respectively and may come from edge and face contacts between SiC semi-conducting particles.

## I. Introduction

Silicon Carbide (SiC) is one of the materials exhibiting excellent features for many applications due to its physical and thermo-electrical properties to operate in harsh environments like high temperature and high electric field [1]. Its semiconducting electronic properties has been used as surge-arresters since the early 1930s to guard lines from lightning [2]. Such arresters were made of polycrystalline ceramics. The non-linear mechanism of conduction is governed by grain boundaries resulting from the sintering of SiC grains [3]. Surface states located at the edge of the grains lead to an electronic band bending, similar to Schottky (metal-semiconductor) barriers in conventional semiconductors. This results in a non-linear dependency of the conductivity with the electric field : the conductivity increases by several orders with the field. Beyond this ceramic electronic component, the idea to load resins with silicon carbide powders has emerged. The intension was of transferring the nonlinear properties of the non-linear interface fillers to a subsequent polymer resin and obtaining semiconducting coatings. Varnishes so produced were useful in reducing corona discharges, *i.e.* ionization of air surrounding a conductor carrying high voltage, thereby reducing insulation degradation [4]. Electrical measurements on plain SiC powders with angular and round SiC particles have been systematically studied [5]. The potential barrier appearing at the grain surface results from surface charging of the semi-conducting SiC grains. The chemical origin is not well understood. A thin inevitable oxide layer, another material or just surface (interface) states, might be at the origin of the electronic band bending [6]. Few is known on the SiC raw material used in commercial anti-corona protection and the way there are formulated: grain size, size distribution, grain shape, chemical composition and concentration [7–8]. To conduct qualification tests of such materials current-voltage measurements are the most widely used method for selecting the appropriate material in order to achieve the desire electrical properties.

Today, SiC composites are used in cable accessories, usually around 88wt.% (~70vol.%), as varnishes *e.g.* in rotating electrical equipment such as power generators [9] or stator winding coils of large turbine-generators [10–11]. According to the percolation theory, around 16 vol.% of spherical particles are required in a continuous network in three-dimensional medium randomly packed [12]. Since the density of SiC is significantly higher compared to the polymer matrix (3210 kg.m<sup>-3</sup> versus 1100 kg.m<sup>-3</sup>), the composites need to be filled with at least 50 wt.% of particles (~24 vol.%). The law near percolated state can be written as:  $\sigma_{\text{composite}} = \sigma_{\text{SiC}} (f_{\text{SiC}} - f_c)^t$ , where  $\sigma_{\text{composite}}$  and  $\sigma_f$  are the conductivity of the composite and the conductive filler respectively,  $f_{\text{SiC}}$  and  $f_c$  are the actual and critical filler volume fraction respectively and  $t$  is the critical exponent. If  $f_{\text{SiC}} < f_c$ , a conduction path (long-range connectivity) is not likely to exist and if  $f_{\text{SiC}} > f_c$  a path is in great potential to form. The percolation characteristics of nonlinear composites dielectrics are different from the traditional conducting composites:  $f_c$  is relatively high, up to 33 vol.% [12]. Secondly, when the field is relatively high, some fillers begin to present nonlinear property *i.e.* beginning to be more conductive due to the local amplified electrical field, leading to a heterogeneous electric field distribution in the volume of the dielectric. The topic is even more complicated since SiC is a very hard material and when crushed, the grains get an angular shape with sharp edges. This results in that mixtures containing angular SiC grains have a conductivity displaying two percolation thresholds obtained at volume fractions of about 25 and 40 vol.%, respectively [5]. These

values are higher than what is predicted in theory 14 vol.% and 31 vol.% for random particles on a cubical lattice [13]. Two types of contacts between angular conductive particles: edge and face connections may explain this phenomenon. However, the experimental work presented in [7–8] shows only a percolation at a fraction of 0.4 vol.% at 300V/mm and only one percolation threshold at a fraction of about 0.25 vol.% at 1kV/mm. This experimental work did not show the two percolations for a given electric field.

In this paper, we report dielectric properties of composites made of SiC filler in polydimethylsiloxane ( $[\text{Si}(\text{CH}_3)_2\text{-O}]_n$ ; PDMS) and show that the critical filler volume fraction is achieved for a concentration of 17 and 24 vol.% at any electric field. Beyond the DC electric characterization, the percolation is studied by impedance spectroscopy based on the dependence of the real permittivity with the filler concentration.

## ii. Materials And Methods

Composites were formed from a two-component silicone elastomer supplied by *Bluestar™ silicones* which cures by a polyaddition reaction catalyzed by a chlorine platinum salt at room temperature after about 24 hours. The elastomer is supplied as a two-part liquid component kit. These parts need to be mixed at 10:1 by weight respectively to make a silicone polymer matrix for the composites defined by its completely inorganic main-chain backbones:  $[\text{Si-O}]_n$ . The SiC employed was a doped industrial  $\beta$ -crystal structure grade with a particle size of 26  $\mu\text{m}$ . The errors due to the weighing of viscous materials are of the order of  $\pm 0.05$ , *i.e.* less than 0.25%. The SiC powders were used as received in the composite materials. The desired filler concentrations were first mixed into the base resin by dual asymmetric centrifugal mixing which ensures a highly efficient mixing at about 3–5 mPa vacuum. Silicone-SiC composite materials were prepared by compression molding at 150°C under pressure 150 bar (15 MPa) for 15 minutes in a plate vulcanization machine. Various Silicone-SiC composite materials were fabricated using a steel die with a thickness of 1 mm and a lateral size of 114 x 80 mm as backing and confining material. The composite samples were then stored in a vacuum drier for testing (24h maturation at room temperature). Table 1 lists the prepared specimens.

Table 1  
Weight and volume experimental concentrations ( $\pm 0.02$ ) of the prepared specimens.

Targeted	5	10	15	20	25	30	35	40	45	50	55	60
Wt.%	5.05	9.97	15.04	20.04	25.03	30.02	34.98	39.93	44.93	50.04	55.00	60.05
Vol.-%	1.66	3.40	5.32	7.38	9.72	12.00	14.61	17.44	20.59	24.14	27.97	32.32

DC volume conductivity investigations were performed using an electrometer (*Keithley 6517B*) associated to a resistivity chamber which shields the sample from electrostatic interference. The chamber is equipped with two conductive flexible electrodes enhancing surface contact between the sample and the electrode. The cathode is guarded to prevent surface leakage currents from being added into the measurement following ASTM D257 requirements. The resistance was measured by applying DC 200V voltage steps followed by short-circuit (samples were subjected to zero voltage) while the polarization and the depolarization currents were continuously monitored during 1800 s. The resistance was calculated using the stable portion of the charging current curve and the average electrical field was assumed to be the applied voltage divided by the inter electrode distance. The tested areas were about 7854 mm<sup>2</sup>. For the sake of accuracy, a single one Keithley electrometer test was conducted on each formulation after elaboration immediately after elaboration.

Assuming a parallel resistor–capacitor circuit, the permittivity of the composites was measured by a broadband dielectric spectrometer, *Novocontrol Alpha-N* high resolution dielectric analyser, over a frequency range from  $10^2$  Hz to 1 MHz with an applied AC voltage of 1Vrms. The temperature was increased from 133K to 353K in intervals of 40K. The experiments were implemented from 133K to 353K.

The particle size distribution of the SiC grains was analyzed using a *Zetasizer* from *Malvern Panalytical*. The SiC powders were dispersed ultrasonically in aqueous medium, and then, the particle size was assessed. Morphological analysis was carried out using a *JEOL 5600 SL* Scanning Electron Microscopy (SEM). A small amount of the powder was deposited on a 12.5 mm-diameter aluminum stub covered with conductive carbon tape. A thin layer of gold (several nm) was deposited by sputtering prior the observation. Morphological characterization of the fillers was done using a field emission scanning electron microscope (FESEM) from *FEI Quanta 200* (*Carl Zeiss, Germany*). The specimens were prepared by both techniques: i) deposition of the raw powder on a conductive support. Most of the images were observed under 1–10 kV acceleration voltage.

The textural properties of carbon fillers were determined using the Brunauer–Emmett–Teller (BET method) by  $N_2$  adsorption measured at 77 K using a BET specific surface area analyzer by *Micromeritics ASAP 2010* automatic physisorption analyzer with multi-gas option, all samples were outgassed at 110 °C under vacuum 24 h beforehand.

DSC tests were conducted on *Mettler Toledo DSC1* in a range of temperatures – 150 to 100°C with a heating rate of  $10^\circ\text{C min}^{-1}$  under a stream of nitrogen (200 mL per min) (*ICGM-CNRS A. Geneste*). All materials were previously dried under vacuum. The DSC capsules containing the sample were drilled in order to avoid any variation in pressure within the capsule, on evaporation of adsorbed phases. After cooling the specimen at about  $-30^\circ\text{C/min}$  from room temperature at  $-150^\circ\text{C}$ , a first heat consists from  $-150^\circ\text{C}$  to  $100^\circ\text{C}$  at  $10^\circ\text{C/min}$ ., a second cooling from 100 to  $-150^\circ\text{C}$  at  $-10^\circ\text{C/min}$ ., an isotherm during 15 minutes at  $-150^\circ\text{C}$  and eventually a second heat from  $-150$  to  $100^\circ\text{C}$  at  $10^\circ\text{C/min}$ . The data reported are obtained during the second heat.

## **iii. Results**

### **III.1. Matrix and filler characterization**

#### **III.1.1. Differential scanning calorimetry analysis of Silicone-SiC composites**

A differential scanning calorimetry (DSC) of silicone matrix is presented in Fig. 1. The glass transition temperature ( $T_g$ ) is  $-124.85^\circ\text{C}$  with a standard deviation of  $2^\circ\text{C}$  (obtained by testing 3 specimens). This low temperature guarantees the invariability of the mechanical properties of the composition, even when used at low temperatures.  $T_g$  low temperature value is in line with the last review paper on PDMS :  $-123^\circ\text{C}$  [14–16],  $-125^\circ\text{C}$  [17]  $-114^\circ\text{C}$  [18–19],  $-110^\circ\text{C}$  [20].  $T_g$  yields insights into the fundamental changes in polymer chain dynamics. The glass transition temperature of polymer composites depends on the free volume of the polymer, the freedom of molecular motion and/or the degree of crosslinking which is affected by the amount of interaction between the polymer and filler particles [18]. No significant change was observed in  $T_g$  of pure silicone and silicone with loading of SiC up to 55 wt.% (Table 2).

Table 2  
DSC results relative to the neat polydimethylsiloxane (PDMS) and the composites concentrated at 40 wt.% up to 55 wt.%.

2nd run	PDMS	40 wt.	45 wt.	50 wt.	55 wt.
T Glass transition (°C)	-124.85	-123.87	-125.48	-126.64	-125.07
T Crystallization (°C)	-93.02	-81.68	-92.18	-93.01	-83.52
$\Delta H_c$ (Jg <sup>-1</sup> )	2.84	3.06	1.59	1.46	1.72
T melting (°C)	-48.75	-47.21	-49.22	-49.54	-47.06
$\Delta H_m$ (Jg <sup>-1</sup> )	-12.18	-2.14	-4.9	-4.72	-2.87

Within experimental error, the crystallization and melting behaviors are essentially the same, which indicates that different SiC filler contents do not apparently chemically interact with the silicone matrix.

On heating above the glass transition ( $T_g$ ), a first cold crystallization peak is observed during warming-up at -93.02°C with an energy of 2.84 Jg<sup>-1</sup>. This suggests that polymer chains have recovered enough mobility. The second peak at -48.75°C is an endothermic melting peak with an energy of -12.18 Jg<sup>-1</sup>. This peak corresponds to a mixture of the melting of the crystalline structure resulting from the cooling of the resin and the cold crystalline structure. It is worth noticing that during our review of literature, we found that the vast majority of studies used Sylgard™ silicone. Both Sylgard 184 [18] and 186 [16] PDMS seems not showing any cold crystallization on heating suggesting that such PDMS have an amorphous structure which is not sufficiently mobile above the  $T_g$  for crystallization to occur. In such case, the endothermic melting peak corresponds to only a single crystalline structure.

### III.1.2. SiC powder analysis

SEM images of the SiC powder is shown in Fig. 2\_A. It appears that grains have an angular shape with sharp edges and rather flat surface which are typical of hard ceramic having been crushed. The particles are well dispersed without apparent formation of agglomerates.

The average and median diameter of the grain has been assessed by laser diffractometry (Fig. 2\_B) to  $26 \pm 1 \mu\text{m}$  and  $20 \pm 1 \mu\text{m}$  respectively. It is worth to notice that sonic dispersion gives the same results suggesting that the SiC particles do not agglomerate and confirm the SEM observations. The dispersion assessed by the ratio of the average

$$\frac{\phi_{\text{average}}}{\phi_{\text{maxi.}}} \sim 0.26.$$

diameter to the largest diameter:

The specific surface area (BET) did not show any detectable surface, the powder being dried at 110°C during 24 hours at low pressure.

The SEM picture of the surface of the composite suggest that SiC particles are statistically evenly distributed.

## III.2. Electric characterization

### III.2.1. DC characterization

The vector equation,  $\vec{J} = (\alpha) \vec{E}$ , describes the electric current locally at any point within a given material. Assuming a heterogeneous medium as homogenous material with a geometry such that its thickness, the cross section through which the charges flow per unit time are known with micron accuracy, experimental J function of E may be reported as:

$$J = k E^\alpha$$

k being an adjustable parameter.

From this equation, nonlinear  $\alpha$  coefficient is calculated:  $\alpha = \frac{\log \frac{j_2}{j_1}}{\log \frac{E_2}{E_1}}$  assuming that  $\alpha(E)$  does not depend on the field in a definite range. This range might be between 0.1 and 1 mA.cm<sup>-2</sup> for instance in the case of varistor ceramics [21].

For composites materials, this formula is adapted as  $\rho(E) = k E^{1-\alpha}$  (i)

Several alternative equations have been proposed in the review of Taylor [22]. However, a better fit seems to be obtained with the equation (ii) [23–25]:

$$\rho(E) = \rho_0 \exp(-nE^\beta) \text{ (ii)}$$

where  $\rho_0$  the resistivity at low field,  $n \sim 0.008$  and  $\beta \sim \frac{1}{2}$  [23].

The  $\rho(E)$  characteristic of our samples are reported in Fig. 3 in a log-log graph. At high filler concentration, it appears that SiC particles decrease the resistivity by about 6 orders while inducing a negative dependence of the resistivity with the field. The resistivity at low field (200V/mm) decreases with the filler concentration. Three sets of resistivities behaviors are observed depending on the electric field: samples with low concentration 1.66% to 17.44 vol.%, their plotting lines are quite horizontal meaning a linear law with  $\alpha \sim 1$  in equation (i) (except for the 17.44 vol% sample at field higher than 800V/mm. This behavior will be discussed below). From 20.59 to 24.14 vol.%, the strong negative slope reveals a higher non-linearity  $\alpha$  coefficient. Finally, the highest concentrations of 27.97 and 32.32 vol% presents a lower negative slope. We can deduce the general rule: for low concentration of SiC (< 15 vol.%), the dependence of the resistivity with the electric field is weak. At about 17 vol.% the non-linearity resistivity appears triggered by high electric field suggesting that 17 vol.% corresponds to a first percolation threshold. Finally, a fair nonlinearity (a decrease of 3 orders of resistivity with the field) has been measured for 2 groups of two specimens each: 21 and 24 vol.% and 27.97 and 32.32 vol.%, suggesting that 24 vol.% matches with a second percolation threshold. The two apparent critical volume fractions are in fair agreement with the theory: 17 versus 14 vol.% and 24 vol.% versus 31 vol.% [13]. A more even dispersion of the fillers would give a better agreement with the experiments.

Figure 4 compares in more details the behavior of specimens which exhibit nonlinearity: samples loaded with 24.14 vol.% and 32.32 vol.%. Experimental data fit better with equation (i) from which the exponent  $1 - \alpha$  has been calculated. The nonlinear  $\alpha$  coefficient is about  $\alpha \sim 5.3$  at 24.13 vol.% and 4.3 at 32.2 vol.% respectively. This shows that the nonlinearity exponent  $\alpha$  depends on the resistivity at low field. Lowering the resistivity leads to decrease the nonlinearity alpha exponent. This suggests that the value of resistivity of the composite saturates at about  $10^8 \Omega.m$ .

Figure 5 reports our specimen with the lowest resistivity (32.32 vol.%) confronted to the data found in the literature. The apparent wide range of the experimental data results from grain size, size distribution and even intrinsic conductivity of SiC as wide bandgap semi-conductor n (N doped) or p (Al and/or B doped) [5]. Our resistivity measurement are 2 orders more resistive than [6;26]. However, in the present study, we reached saturation at about 35 vol.% limited by the viscosity of the SiC/silicone mixture. This might be correlated by the semi-crystalline silicone matrix carried out in the present work.

With an aim of identifying any apparent experimental percolation threshold we have reported in Fig. 6 the conductivity as a function of the filler loading in the range 0.2 and 1.0 kV/mm. The conductivity is found to increase seven decades from 1.66 vol.% to 32.20 vol.%. A significant change in conductivity - at least two decades - is presumably related to a percolation threshold.

Based on this definition, two percolation thresholds may be observed at about 17 vol.% and 24 vol.% (Fig. 6). The first threshold is more evident at high field (1kV/mm), the second one more evident at low field (200V/mm).

At 400V/mm, both percolation thresholds are identified as the theory foresees [5]. It is worth noting that only one threshold was so far identified experimentally for a given field. A single threshold at high volume fraction at 200V/mm and an unique threshold at low volume fraction at 1kV/mm have indeed been reported [5].

## III.2.2. Real permittivity

### III.2.2.1 Real permittivity in frequency domain

Figure 7 shows the evolution of the permittivity according to the frequency in the range 0.02 to 1 MHz for SiC filled PDMS. The value of the composite permittivity is found between the permittivity of the neat silicone resin and the SiC powder. The permittivity increases at low frequency, suggesting an increasing influence from DC conduction at the lowest frequencies. From 1MHz to about 1kHz, the permittivities are independent of the frequency for all samples.

### III.2.2.1 Real permittivity at 1kHz with the volume fraction

Effective Media Theory (EMT) [28] has been developed to produce acceptable approximations to describe effective macroscopic permittivity of micro-inhomogeneous medium such as composite [28]. Mixtures of dielectrics can be considered on the basis of layer materials with the layers in the parallel or normal to the applied field. When layers are parallel to the capacitor plates, the microstructure corresponds to capacitive elements in series and the permittivity of the mixture or the composite can be expressed as:

$$\frac{1}{\epsilon_{\text{composite}}} = \frac{f_{\text{SiC}}}{\epsilon_{\text{SiC}}} + \frac{1-f_{\text{SiC}}}{\epsilon_{\text{Silicone}}}$$

In contrast, when the plates elements are arranged normal to the capacitor plates, the capacitance are additive:

$$\epsilon_{\text{composite}} = f_{\text{SiC}} \epsilon_{\text{SiC}} + (1-f_{\text{SiC}}) \epsilon_{\text{silicone}}$$

Experimental values should be intermediate values between these two configurations. For instance, a rule of mixture for spherical particles dispersed and isolated in a silicone matrix may be expressed as:

$$\epsilon_{\text{composite}} = \frac{(1-f_{\text{SiC}})\epsilon_{\text{silicone}}\left(\frac{2}{3} + \frac{\epsilon_{\text{SiC}}}{3\epsilon_{\text{silicone}}}\right) + f_{\text{SiC}}\epsilon_{\text{SiC}}}{(1-f_{\text{SiC}})\left(\frac{2}{3} + \frac{\epsilon_{\text{SiC}}}{3\epsilon_{\text{silicone}}}\right) + f_{\text{SiC}}}$$

On Fig. 8, experimental data diverge from the EMT theory at the critical concentration of 17 vol.% : the first percolation threshold. This suggests to us that this is a departure from the mixture rules: SiC particles cannot be no longer considered as isolated, suggesting the formation of a long-range connectivity.

## Iv. Conclusion

An investigation has been performed to study the nonlinear I-V mechanism with the filler content of a SiC/silicone resin composite. The resistivity depends on the electric field with a power law :  $\rho(E) = k E^{1-\alpha}$  with  $\alpha \sim 4$ . Two apparent critical



concentrations at about 17 and 24 vol.% (percolation thresholds) are observed with respect of the electric field. These sharp conductivity changes may be related to a mechanism of conduction through the edge contacts and through the face contacts of the SiC crystals. The permittivity of the tested composites increases up from 3.2 at 8 vol% to 6 at 17 vol% and reaches 12 at 32.2 vol.%. At the first critical concentration (17 vol.%) a departure from effective media theory is observed suggesting that the particles cannot be considered as isolated in the silicone matrix.

## Declarations

### Ethics approval

This work follows ethical standards

### Funding

This work was supported by Schneider Electric

### Competing Interests

The authors have no relevant financial or non-financial interests to disclose

### Author Contributions

Hocine Merini, Jean-Michel Reboul, Jean-Louis Bantignies, Mehrdad Hassanzadeh and Renaud Metz contributed to the study conception and design. The first draft of the manuscript was written by Renaud Metz. Hocine Merini, Jean-Michel Reboul, Jean-Louis Bantignies, Mehrdad Hassanzadeh commented on previous versions of the manuscript.

### Acknowledgement

Part of the elaboration work was done in *Polytech Montpellier*, a French engineering College. Thanks to Calypso Baril and Béatrice Galland from the *Materials Science and Engineering* department for the access to the elaboration equipment and Samuel Pauletto, *IUT Montpellier* for his help in preparing the specimens.

### Availability of data and materials

The experimental data of this work are available on the following link:  
<https://cloud.coulomb.umontpellier.fr/index.php/s/xzsb4yT4x8p9NBR>

### Ethics approval

Not applicable

### Consent to participate

Not applicable

### Consent for publication

Not applicable

## References

1. Papanasam E, Prashanth Kumar B, Chanthini B, E. Manikandan, Lucky Agarwal (2022) A Comprehensive Review of Recent Progress, Prospect and Challenges of Silicon Carbide and its Applications, *Silicon* 14, 12887–12900
2. Grisdale RO (1940) Silicon Carbide Varistors. *Bell Laboratories Record* 19: 46-51.
3. Ove FS (2012), Charakterisierung der nichtlinearen Widerstandseigenschaften von Endenglimmschutzsystemen rotierender Hochspannungsmaschinen. *Elektrotechnik & Informationstechnik*. 129/5: 306–313.
4. Electric stress-grading coatings (1962) US patent 3210461.
5. Nettelblad B, Martensson E, Onneby C, Gäfvert U, Gustafsson A (2003) Two percolation thresholds due to geometrical effects : experimental and simulated results. *J. Phys. D: Appl. Phys.* 36 : 399–405.
6. Donzel L, Greuter F, Christen T (2011) Nonlinear resistive electric field grading Part 2: Materials and applications. *IEEE Electrical Insulation Magazine*, March/April, 27, 2 : 18-29.
7. Onneby C, Martensson E, Gafvert U, Gustafsson A, Palmqvist L (2001) Electrical Properties of Field Grading Materials Influenced by the Silicon Carbide Grain Size. *IEEE 7<sup>th</sup> International Conference on Solid Dielectrics*, June 25-29 Eindhoven. the Netherlands : 43-45.
8. Martensson E (2003) Modelling electrical properties of composite materials, Thesis, Kungl Tekniska Högskolan, Trita-ETS-2003-10, ISSN-1650-674x, Stockholm, Sweden.
9. Conley DJ, Frost N (2005) Fundamentals of semi-conductive systems for high voltage stress grading. *Proceedings Electrical Insulation Conference and Electrical Manufacturing Expo.*: 89-92.
10. Staubach C, Kempen S, Pohlmann F (2011) Calculation of electric field distribution and temperature profile of end corona protection systems on large rotating machines by use of finite element model. *IEEE International Symposium on High Voltage Engineering*, Hannover, Germany, August 22-26.
11. Staubach C, Kempen S, Pohlmann F (2010) Electrical-thermal optimization of end corona protection systems on large rotating machines by use of numerical optimization algorithm based on FEM. *IEEE International Symposium on Electrical Insulation*, 6-9 June, San Diego, CA, USA
12. Yang X, Hu J, Chen S, He J (2016) Understanding the Percolation Characteristics of Nonlinear Composite Dielectrics. *Nature, Scientific reports*, 6:30597:1-10.
13. Bunde A, Havlin S (ed) (1991) *Fractals and Systems* (New York: Springer)
14. Zalewski K, Chylek Z, Trzcinski W (2021) A review of polysiloxanes in terms of their application in explosives, *Polymers*, 13, 1080 : 1-11.
15. Shi X (2021) The crystalline structure of polydimethylsiloxane : additional results and additional questions, PhD, Paris-Saclay, 15 Januar.
16. Gupta NS, Lee KS, Labouriau A (2021) Tuning Thermal and Mechanical Properties of Polydimethylsiloxane with Carbon Fibers. *Polymers* 13: 1141.
17. Adachi H, Adachi K, Ishida Y and Kotaka T (1979) Dielectric relaxation of polydimethylsiloxane. *Journal of polymer Science : Polymer Physics Edition*, 16 : 851-857.
18. Xu J, Razeeb K, Roy S (2008) Thermal Properties of Single Walled Carbon Nanotube-Silicone Nanocomposites. *Journal of Polymer Science: Part B: Polymer Physics*, Vol. 46, 1845–1852 :1845-1852.
19. Raza MA, Westwood A, Brown A, Hondow N, Stirling C (2011) Characterization of graphite nanoplatelets and the physical properties of graphite nanoplatelet/silicone composites for thermal interface applications. *Carbon* 49 : 4269-4279.
20. Zhao J, Chen P, Lin Y, Chen W, Lu A, Meng L, Wang D, Li L (2020) Stretch-Induced Intermediate Structures and Crystallization of Poly(dimethylsiloxane): The Effect of Filler Content. *Macromolecules* 53: 719-730.

21. Metz R, Boudhen L, Tahir S, Phou T, Prevot G, Jelinek R, Dieudonne P, Hanssazadeh M (2017) Recycling zinc oxide varistor blocks for electro-active silicone composites. *Int J. Appl Ceram Technol.* 2017.
22. Taylor N (2006) Diagnostics of stator insulation by dielectric response and variable frequency partial discharge measurements, Tech. rep., Royal Institute of Technology, KTH, 2006. Licentiate Thesis.
23. Merouchi A, David E, Baudoin F, Mary D, Fofona I (2015) Optimization of the electrical properties of epoxy-SiC composites for stress-grading application. Annual Report Conference on Electrical Insulation and Dielectric Phenomena, Ann Arbor, Michigan. USA. October 18–21, 2015.
24. Vanga-Bouanga C, Heid TF, David E, Frechette MF, Savoie S (2013) Tailoring of the electrical properties of silicon carbide for field grading application. Electrical Insulation Conference, Ottawa, Ontario, Canada 2-5 June 2013, 263-66.
25. Merouchi A (2016) Caractérisation de revêtement anti-effluve à base de carbure de silicium pour les machines haute tension, PhD, Montréal, Canada, 4 Mars 2016.
26. Espino-Cortes FP, Jayaram SH, Cherney EA (2005) Stress grading materials for cable terminations under fast rise time pulses. IEEE Annual report conference on electrical insulation and dielectric phenomena, 19 December 2005, Nashville, TN, USA : 621-24.
27. Martensson E, Nettelblad B, Gäfvert U (1998) Electrical properties of field grading materials with silicon carbide and carbon black. IEEE International Conference on conduction and breakdown in solid dielectrics, 22-25 June, Västerås, Sweden : 548-552.
28. Wang J, Carson JK, North MF, Cleland DJ (2008) New structural model of effective thermal conductivity for heterogeneous materials with co-continuous phases. *International Journal of Heat and Mass Transfer* 51: 2389–2397.

## Figures

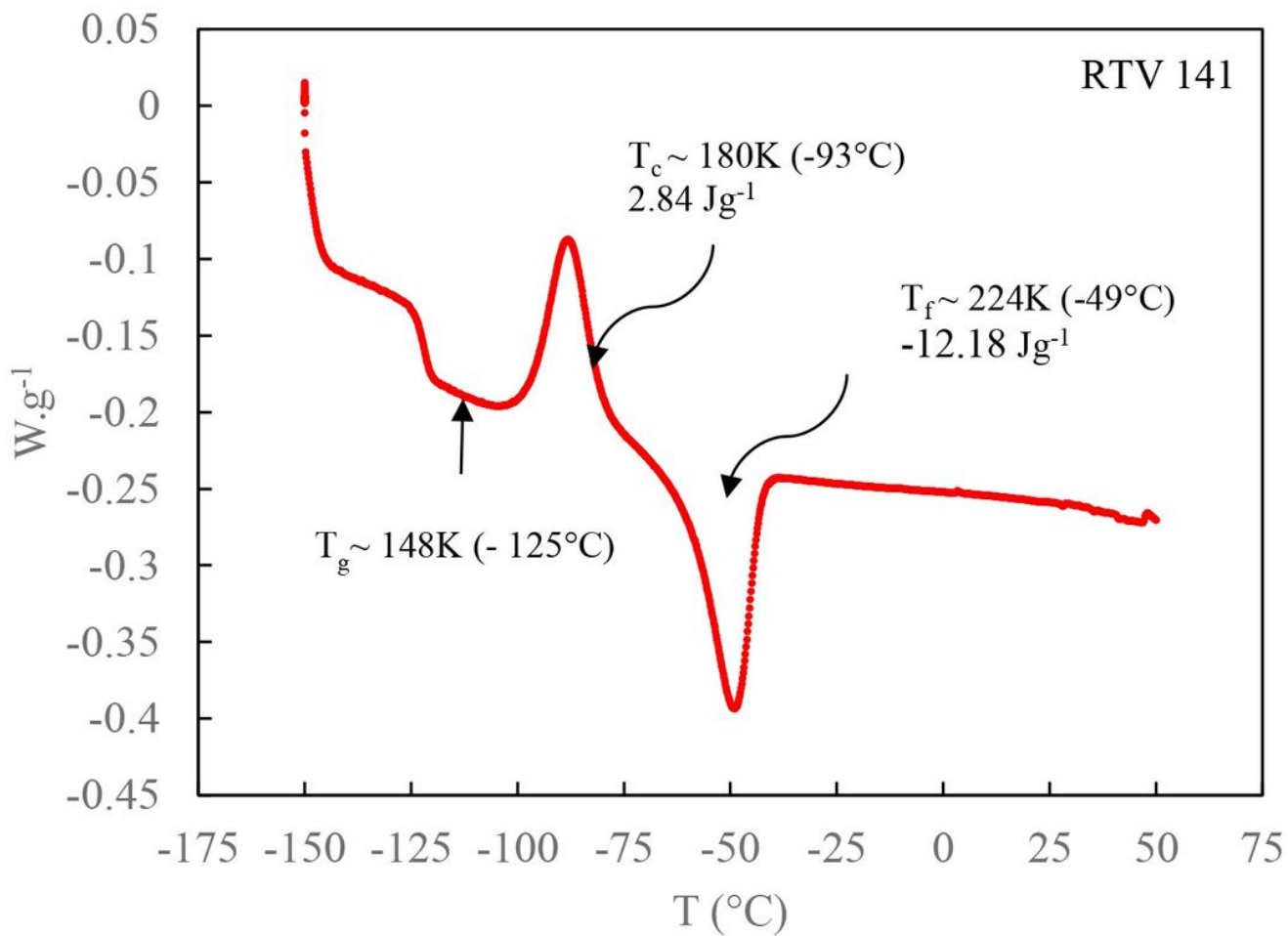
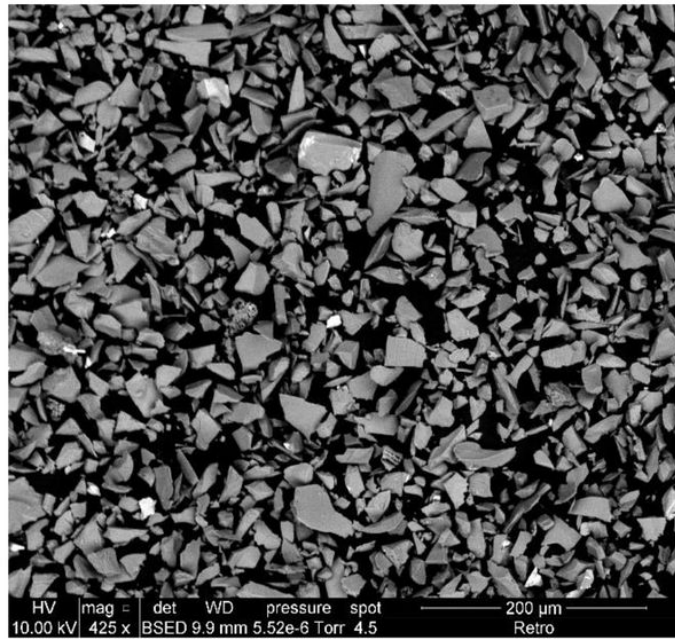


**Figure 1**

DSC heating profile of neat silicone under N<sub>2</sub> at 10°C/minutes with a weight of 6.85 mg – (Glass transition temperature at the inflection point: -122°C)

A



B

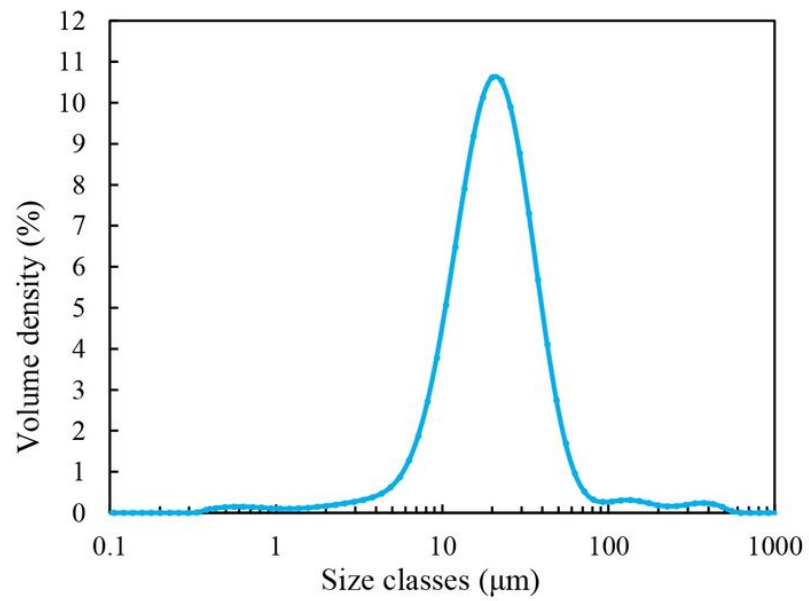


**Figure 2**

Grain morphology and size assessment by scanning electron micrograph (A) and laser diffractometry by volume (B).

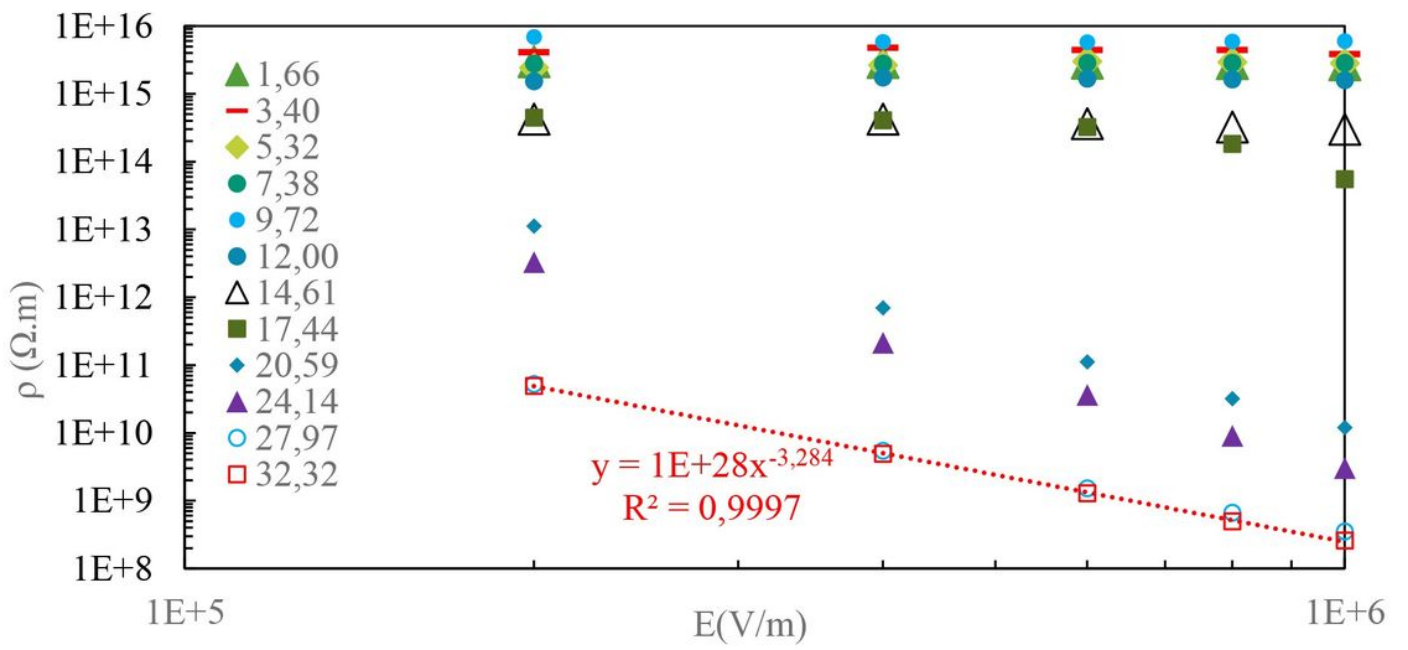


**Figure 3**

Experimental resistivity characteristics of silicone-SiC composite ( $40 \pm 1^\circ C$ ). (Concentrations are expressed in volume).

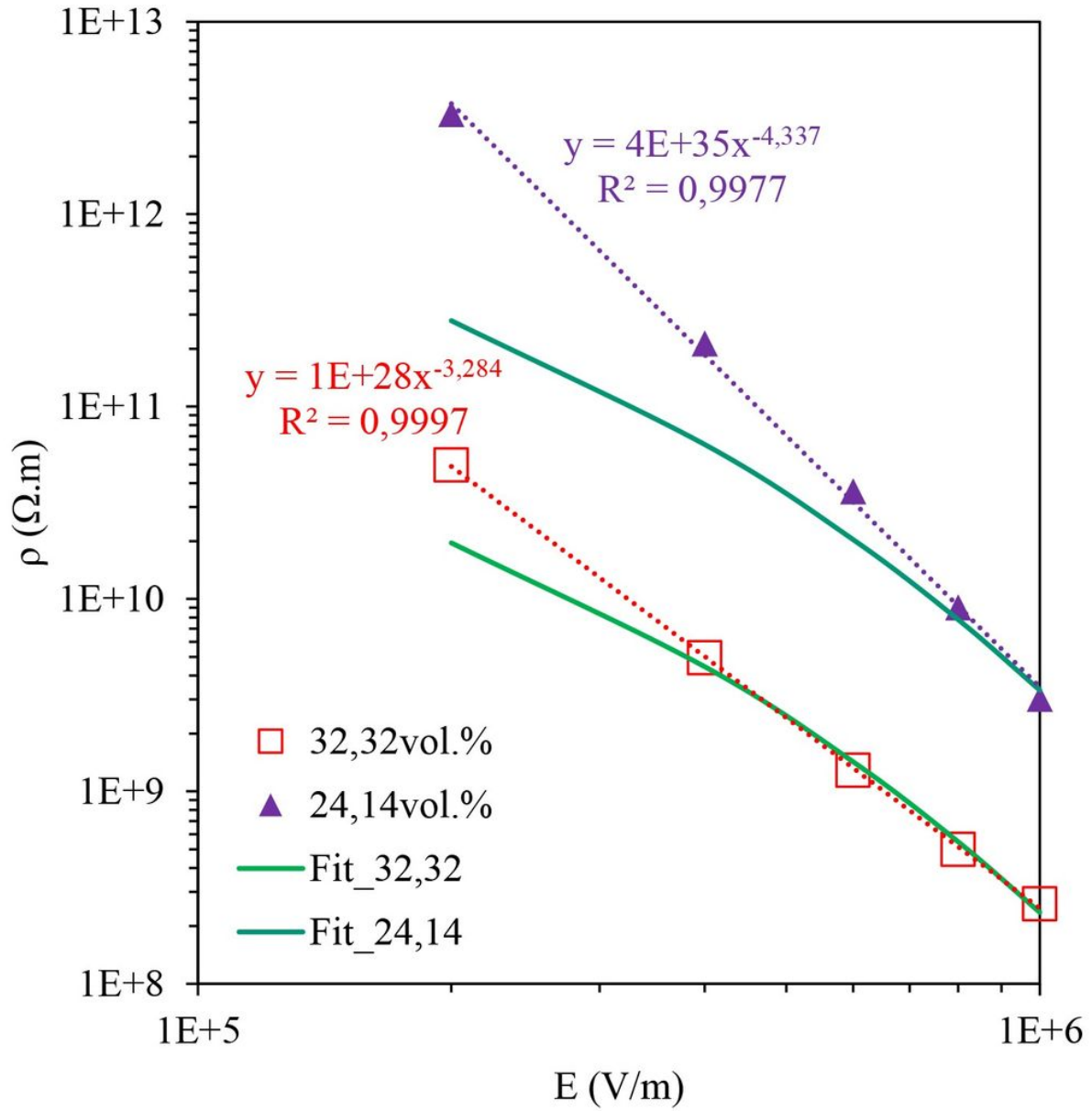


**Figure 4**

Resistivity characteristic RTV141 filled with 32.32 vol.% and 24.14vol.% SiC respectively (Green lines: fit from equation (ii) with  $\rho_0 = 7 \cdot 10^{11} \Omega.m$ .  $n = 0.008$ .  $\beta = \frac{1}{2}$  and  $\rho_0 = 1 \cdot 10^{13} \Omega.m$ .  $n = 0.008$ .  $\beta = \frac{1}{2}$ ).

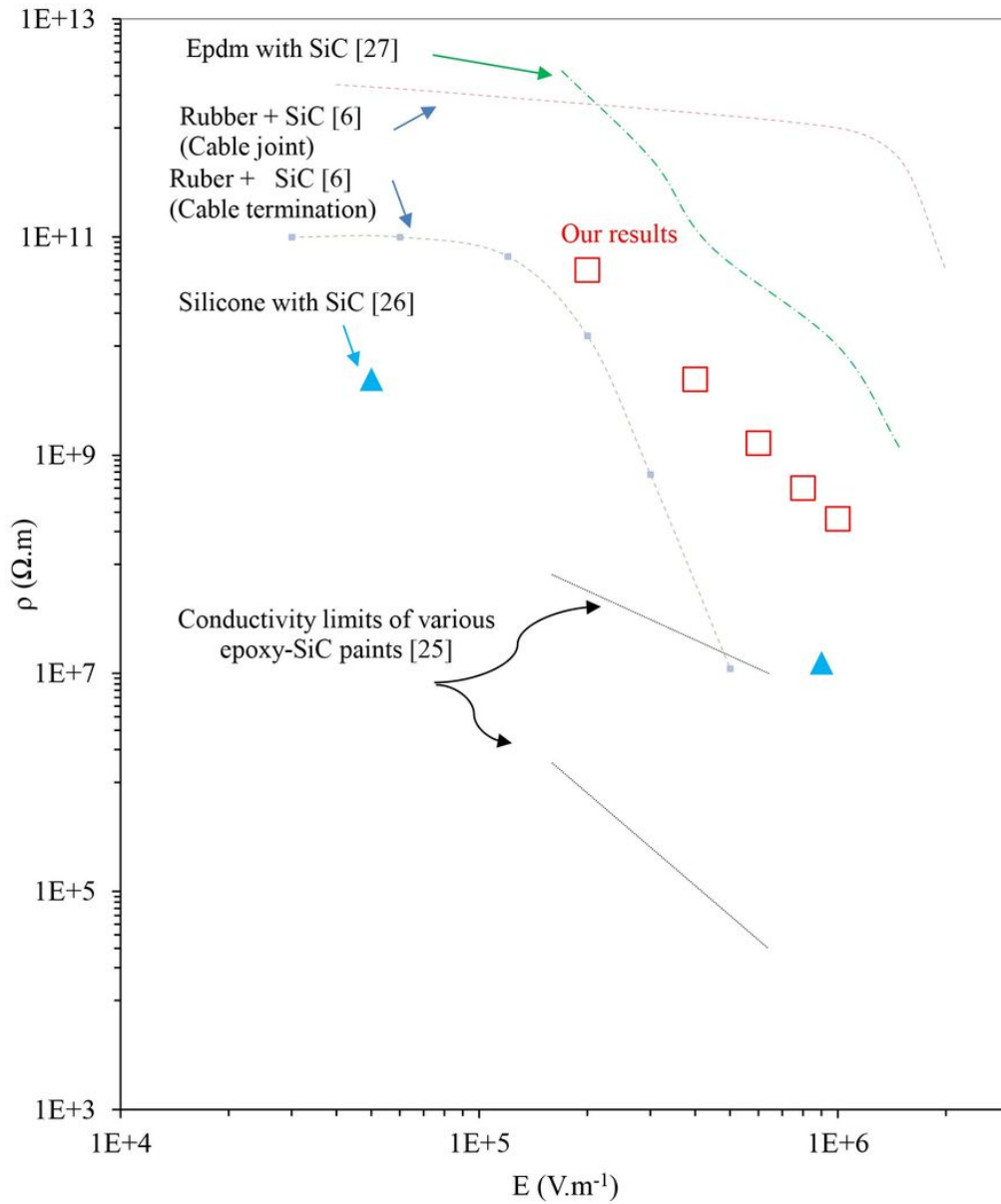


**Figure 5**

Overview of the resistivity range of stress grading materials made of SiC. Dash lines [25] define limits of various epoxy-SiC paints fabricated using a glass plate as backing material. Empty squares : our data at 40°C for 32.2 vol.%. Filled triangles: silicone + SiC (40 vol.% - 23 microns)[26], EPDM + 17.5vol.% SiC (10 microns) + 13.1vol.% Carbon black (1 micron) [27].



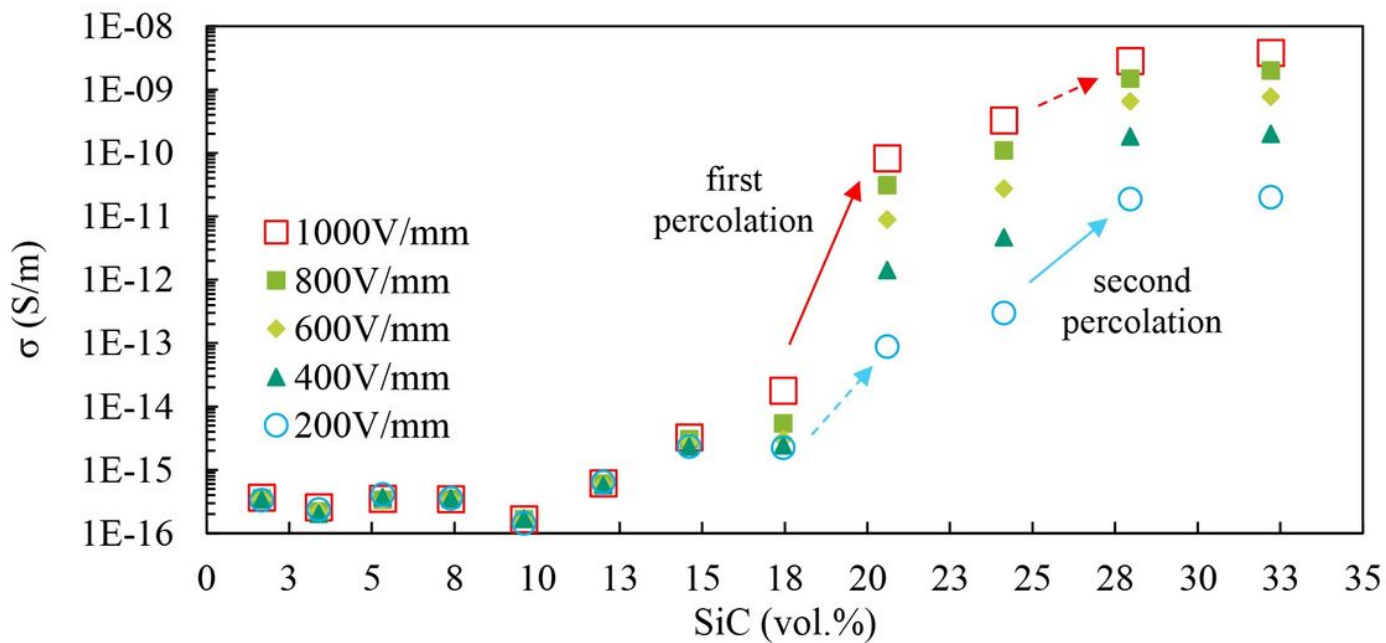


Figure 6

Conductivity as a function of particle concentration measured for silicone filled with SiC grains (1kV/mm DC at  $40 \pm 1^\circ\text{C}$ ).

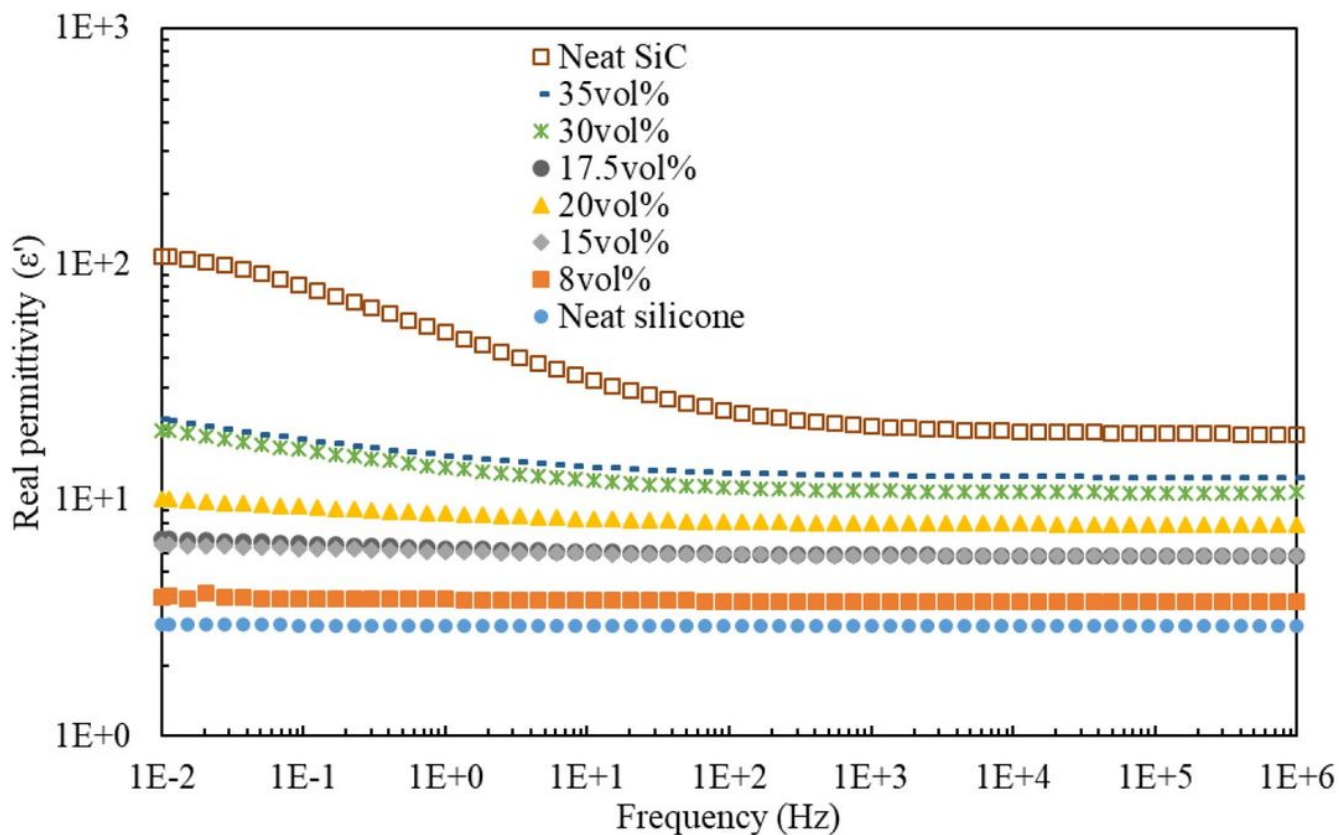
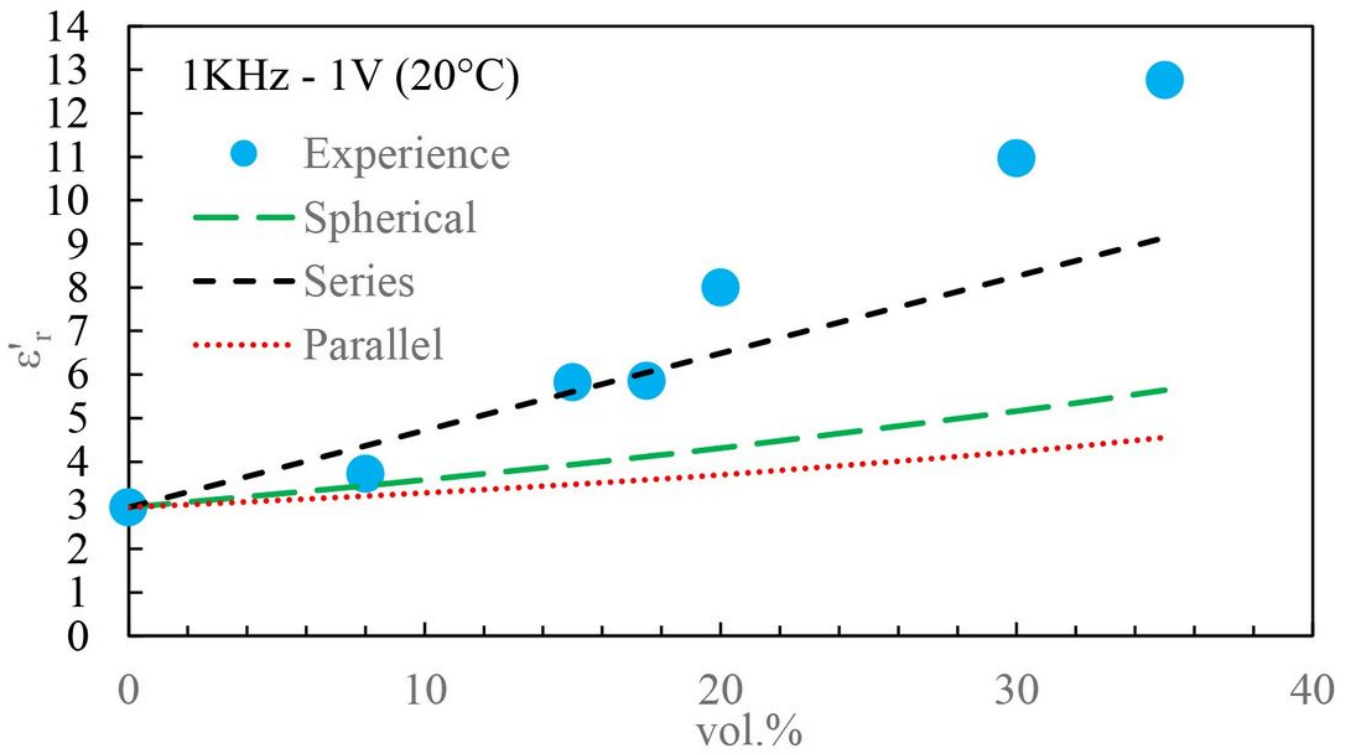


Figure 7

Polydimethylsiloxane at  $20 \pm 1^\circ\text{C}$ . Relative real permittivity *versus* frequency between 0.01 and  $10^6$  Hz.



**Figure 8**

Plot of real permittivity with respect to the concentration of SiC at 50Hz.